

Gaussianity of cosmic velocity fields and linearity of the velocity–gravity relation

Paweł Ciecieląg,^{1★} Michał J. Chodorowski,^{1★} Marcin Kiraga,²
Michael A. Strauss,³ Andrzej Kudlicki^{1†} and François R. Bouchet⁴

¹Copernicus Astronomical Centre, Bartycka 18, 00-716 Warsaw, Poland

²Warsaw University Observatory, Aleje Ujazdowskie 4, 00-478 Warsaw, Poland

³Princeton University Observatory, Princeton, NJ 08544-1001, USA

⁴Institut d’Astrophysique, 98 bis Boulevard Arago, 75014 Paris, France

Accepted 2002 October 18. Received 2002 October 17; in original form 2000 October 31

ABSTRACT

We present a numerical study of the relation between the cosmic peculiar velocity field and the gravitational acceleration field. We show that on mildly non-linear scales (4–10 h^{-1} Mpc Gaussian smoothing), the distribution of the Cartesian coordinates of each of these fields is well approximated by a Gaussian. In particular, their kurtoses and negentropies are small compared to those of the velocity divergence and density fields. We find that at these scales the relation between the velocity and gravity field follows linear theory to good accuracy. Specifically, the systematic errors in velocity–velocity comparisons due to assuming the linear model do not exceed 6 per cent in β . To correct for them, we test various non-linear estimators of velocity from density. We show that a slight modification of the α -formula proposed by Kudlicki et al. yields an estimator which is essentially unbiased and has a small variance.

Key words: methods: numerical – cosmology: theory – dark matter – large-scale structure of Universe.

1 INTRODUCTION

According to the gravitational instability paradigm, structures in the Universe formed by the growth of small inhomogeneities present in the early Universe. Gravitational instability gives rise to a coupling between the density and peculiar velocity fields on scales larger than the size of clusters of galaxies, the largest bound objects in the Universe. On very large, linear scales, the relation between the density contrast δ and the peculiar velocity v in comoving coordinates can be expressed in differential form,

$$\delta(\mathbf{r}) = -(H_0 f)^{-1} \nabla \cdot \mathbf{v}(\mathbf{r}), \quad (1)$$

or in integral form,

$$\mathbf{v}(\mathbf{r}) = \mathbf{g}(\mathbf{r}). \quad (2)$$

Here,

$$\mathbf{g}(\mathbf{r}) \equiv H_0 f \int \frac{d^3 \mathbf{r}'}{4\pi} \frac{\delta(\mathbf{r}')(\mathbf{r}' - \mathbf{r})}{|\mathbf{r}' - \mathbf{r}|^3} \quad (3)$$

is a quantity *proportional* to the gravitational field,¹ expressed in units of km s^{-1} . The coupling constant, f , carries information about the underlying cosmological model, and is related to the cosmological matter density parameter, Ω_m , and cosmological constant, Ω_Λ by

$$f(\Omega_m, \Omega_\Lambda) \simeq \Omega_m^{0.6} + \frac{\Omega_\Lambda}{70} \left(1 + \frac{\Omega_m}{2} \right) \quad (4)$$

(Lahav et al. 1991). Hence, comparing the observed density and velocity fields of galaxies allows us to constrain Ω_m , or the degenerate combination $\beta \equiv \Omega_m^{0.6}/b$ in the presence of galaxy biasing; see, for example, Strauss & Willick (1995) for a review. This comparison is done by extracting the density field from full-sky redshift surveys – such as the Point Source Catalogue Redshift (PSCz) Survey (Saunders et al. 2000) – and comparing it to the observed velocity field from peculiar velocity surveys. The methods for doing this fall into two broad categories. We can use equation (2) to calculate the predicted velocity field from a redshift survey, and compare the result with the measured peculiar velocity field; this is referred to as a velocity–velocity comparison. Alternatively, we can use the differential form, equation (1), and calculate the divergence of the observed velocity field to compare directly with the density field

¹The linear relation between the peculiar velocity and the gravity, $\bar{\mathbf{g}}$, is (e.g. Peebles 1980) $\mathbf{v} = 2f/(3H\Omega_m)\bar{\mathbf{g}}$. For simplicity, here we define the *scaled* gravity, $\mathbf{g} \equiv 2f/(3H\Omega_m)\bar{\mathbf{g}}$. Then equation (2) follows and \mathbf{g} is given by equation (3).

★E-mail: pci@camk.edu.pl (PC); michal@camk.edu.pl (MJC)

†Present address: University of Texas Southwestern Medical Centre, Dallas, TX 75390-9038 USA.

from a redshift survey; this is called a density–density comparison. Non-linear extensions of equation (1) have been developed by a number of workers: Nusser et al. (1991), Bernardeau (1992), Gramann (1993), Mancinelli et al. (1994), Mancinelli & Yahil (1995), Chodorowski (1997), Chodorowski & Łokas (1997), Chodorowski et al. (1998), Bernardeau et al. (1999), Dekel et al. (1999) and Kudlicki et al. (2000, hereafter KCPR); see also the discussion below. However, very little work has been carried out to test on what scales the integral relation, equation (2) holds, and how it might be extended into the mildly non-linear regime; thus the motivation for this paper. Attempts have been made to carry out velocity–velocity comparisons with very large smoothing lengths, e.g. the inverse Tully–Fisher method of Davis, Nusser & Willick (1996), and very small smoothing lengths, the VELMOD method of Willick et al. (1997); Willick & Strauss (1998). Davis, Strauss & Yahil (1991), and more recently Berlind, Narayanan & Weinberg (2000) discuss the systematic errors caused by mismatch of smoothing scales between the velocity and density fields. In this paper, we concentrate on the velocity–velocity comparison after smoothing on scales of $4 h^{-1}$ Mpc or larger; any smaller smoothing would be affected by strongly non-linear effects, while larger smoothing would reduce the number of independent volumes over which the comparison could be made.

The amplitude of the velocity field smoothed on a given scale R with the window W depends on the density field power spectrum, $P(k)$, as

$$\langle v^2 \rangle \propto \int dk P(k) \tilde{W}^2(kR), \quad (5)$$

while for the density field the relation is as follows

$$\langle \delta^2 \rangle \propto \int dk k^2 P(k) \tilde{W}^2(kR); \quad (6)$$

see the discussion in chapter 2 of Strauss & Willick (1995). Here, \tilde{W} is the Fourier transform of the smoothing window. The absence of the k^2 term in equation (5) means that the velocity field is more heavily weighted by modes with low values of the wavenumber k , i.e. large scales which are fully in the linear regime. Therefore, we expect the relation between the velocity, v , and the gravity, g , to be closer to linear than that between the density and velocity divergence.

KCPR have shown that the relation between

$$\theta \equiv -(H_0 f)^{-1} \nabla \cdot v(\mathbf{r}), \quad (7)$$

(see equation 1) and δ [proportional to $\nabla \cdot g(\mathbf{r})$] is non-linear on small scales. They have proposed a semi-empirical formula accurately describing the dependence of $\theta_\delta \equiv \langle \theta | \delta \rangle$ on δ :

$$\theta_\delta = \alpha[(1 + \delta)^{1/\alpha} - 1] + \epsilon. \quad (8)$$

Here, the constant ϵ is introduced in order to keep $\langle \theta \rangle = 0$ as it must; it is approximately

$$\epsilon = \frac{\alpha - 1}{2\alpha} \sigma_\delta^2 + \mathcal{O}(\sigma_\delta^4), \quad (9)$$

where $\sigma_\delta^2 \equiv \langle \delta^2 \rangle$ denotes the variance of the density field. Thus, this approximation to ϵ becomes progressively worse as the fluctuations become more non-linear and in the following we use the exact value of ϵ , obtained numerically. KCPR have found that $\alpha = 1.9$ is a good fit over a large range of smoothing scales. Solving equation (7) for v in the case of an irrotational flow gives

$$v(\mathbf{r}) = \frac{H_0 f}{4\pi} \int d^3 r' \frac{\theta_\delta(\mathbf{r}')(\mathbf{r}' - \mathbf{r})}{|\mathbf{r}' - \mathbf{r}|^3}, \quad (10)$$

where equation (8) gives an expression for θ_δ .

In this paper, we investigate the non-linearities of the relationship between the velocity and gravity fields using a set of grid-based simulations. The simulations are described in Section 2. In Section 3, we ask how well the probability distribution functions (PDFs) of the Cartesian components of v and g are fitted with a Gaussian. Given that the source fields for the velocity and gravity fields (i.e. the velocity divergence and density contrast respectively) have mildly non-Gaussian distributions, it is not a priori obvious what the distribution of the integral quantities should be. In Section 4 we directly measure the relation between v and g on various scales, and test the extent to which linear theory, or non-linear extensions to it, may hold. This is important in determining whether the existing velocity–velocity comparisons which use linear theory give biased results. We present our conclusions in Section 5. Two appendices contain derivations of results used in the text.

2 THE SIMULATIONS

We performed our simulations using the Cosmological Pressureless Parabolic Advection (CPPA) code; see Kudlicki, Plewa & Różycka (1996) and KCPR. Matter in this code is represented as a non-relativistic pressureless fluid, and its equations of motion are solved on a uniform grid fixed in comoving coordinates. Periodic boundary conditions are applied. Parabolic interpolation of the hydrodynamical state – as in the piecewise parabolic method scheme, see Colella & Woodward (1984) – assures low internal diffusion of the code and accurate treatment of high density and velocity gradients.

We chose to use a grid-based code rather than an N -body code, because it produces a volume-weighted velocity field directly. This is important because equation (10) is a solution to equation (7) only when v is a potential (curl-free) field, and the *mass-weighted* velocity field exhibits curl even in the linear regime.² Moreover, the a priori unknown galaxy bias does not allow us to treat observational data as purely mass-weighted anyway.

All our simulations assume an Einstein–de Sitter universe. The relation between the velocity and the (scaled) gravity in the mildly non-linear regime is insensitive to the cosmological density parameter and cosmological constant, as demonstrated both analytically (Gramann 1993; Chodorowski 1997; Nusser & Colberg 1998; see also Appendix B3 of Soccimarro et al. 1998), and by means of N -body simulations (Bernardeau et al. 1999), thus our results should be valid for any cosmology.

Our simulations start from Gaussian density fluctuations with the linear automated plate measurement (APM) power spectrum (Baugh & Efstathiou 1993, 1994; Baugh & Gaztañaga 1996). The initial velocity field is obtained from equation (2). The initial fields are evolved until the linear variance of the density in spheres of radius $8 h^{-1}$ Mpc, σ_8 , is unity. Then for subsequent analysis the output is selected for which non-linear $\sigma_8 = 0.87$; the cluster normalization in the currently preferred model $\Omega_m = 0.3$, $\Omega_\Lambda = 0.7$ (Eke, Cole & Frenk 1996).

In order to test the dependence of the results on the spatial resolution and box size we have studied three numerical models with parameters given in Table 1. To improve the statistics, we have performed six realizations of each of the models, with different random phases of the initial density field. We have also performed a few

²The mass-weighted velocity field is proportional to $(1 + \delta)v$. If its curl is to be zero, with $\nabla \times v = 0$, we would require $\nabla \delta \times v = 0$. There is no a priori reason for this even in the linear regime. The mean value of the cosine of the angle between $\nabla \delta$ and v measured on the $30 h^{-1}$ Mpc scale in our six high-resolution simulations (see Table 1) is 0.81. The directions of these vectors are thus correlated, but not parallel.

Table 1. Parameters of the studied models. Hereafter, the model with the cell size equal to $1.56 h^{-1}$ Mpc will be called the ‘high-resolution model,’ while the remaining models will be called ‘low-resolution models’.

Grid	Box size (h^{-1} Mpc)	Cell size (h^{-1} Mpc)
64^3	200	3.13
128^3	200	1.56
128^3	400	3.13

additional simulations with the time-step reduced five times; the results did not change noticeably.

3 THE MARGINAL DISTRIBUTIONS OF v AND g

The typical correlation length of the density field is of the order of $5 h^{-1}$ Mpc, while g is influenced by density fluctuations in a much larger region. For instance, the gravitational acceleration of the Local Group receives considerable contributions from shells up to at least $150 h^{-1}$ Mpc; see, for example, Rowan-Robinson et al. (2000). Thus, g , and similarly v , come from integration over an effective domain containing a large number of essentially independent regions. Hence, the central limit theorem suggests that they should have close to Gaussian distributions.

We test the Gaussianity hypothesis with our simulations. We plot the measured distribution functions for individual Cartesian components of the peculiar velocity and gravity fields, which we label v and g . It turns out that on mildly non-linear scales, the distributions are well fitted by Gaussians. Figs 1 and 2 show the distributions for $4 h^{-1}$ Mpc Gaussian smoothing. (As there is no preferred direction in space, the distributions must be even functions. Therefore, without the loss of information we plot them as functions of the absolute value of a Cartesian component.) The closeness to a Gaussian distribution is remarkable, especially for the velocity field.

A standard way of quantifying modest departures from Gaussianity is to decompose the PDF with an Edgeworth expansion: a leading Gaussian, plus correction terms with amplitudes proportional to the higher-order connected moments of the field (Longuet-Higgins 1963; Juszkiewicz et al. 1995; Bernardeau & Kofman 1995). As there is no preferred direction in space, the skewness of the PDF of the Cartesian coordinates of the velocity and gravity fields must equal zero. Thus, the first non-vanishing connected moment of a Cartesian component of the velocity field is its kurtosis, $\mathcal{K}_v = (\langle v^4 \rangle - 3\langle v^2 \rangle^2) / \langle v^2 \rangle^2$, and similarly for the gravity field. Therefore, the kurtosis measures the leading-order departure from Gaussianity of the fields (Kofman et al. 1994; Catelan & Moscardini 1994). Specifically, the Edgeworth expansion in our case reads

$$P(\mu) = \phi(\mu) \left[1 + \frac{\mathcal{S}_4 \sigma_\delta^2}{24} H_4(\mu) + \mathcal{O}(\sigma_\delta^4) \right]. \quad (11)$$

Here, $P(\mu)$ is the PDF for the variable v/σ_v or g/σ_g , where $\sigma_v^2 = \langle v^2 \rangle$ and $\sigma_g^2 = \langle g^2 \rangle$ are the variances of the velocity and gravity fields respectively, and $\phi(\mu) = (2\pi)^{-1/2} \exp(-\mu^2/2)$ is the standardized normal distribution. The symbol H_4 denotes the fourth-order Hermite polynomial. The quantity \mathcal{S}_4 is related to the velocity, or gravity, kurtosis and the variance of the *density* field in the following way:

$$\mathcal{K}_v = \mathcal{S}_{4v} \sigma_\delta^2 \quad \text{and} \quad \mathcal{K}_g = \mathcal{S}_{4g} \sigma_\delta^2. \quad (12)$$

The quantities \mathcal{S}_{4v} and \mathcal{S}_{4g} are called hierarchical amplitudes. For a given smoothing scale, during the weakly non-linear evolution

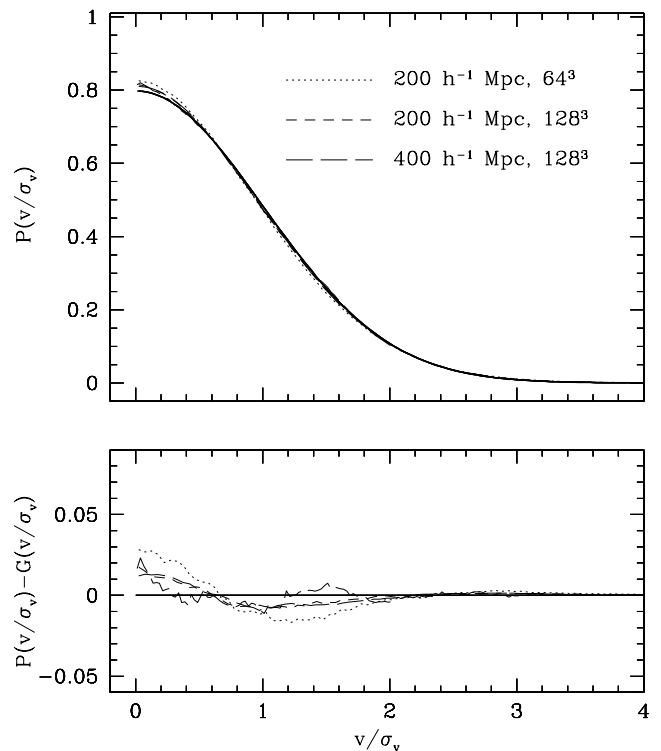


Figure 1. The probability distribution of a Cartesian component of the $4 h^{-1}$ Mpc Gaussian-smoothed velocity field from our simulations and its deviations from Gaussianity. In both panels, the dotted line represents the results for the 64^3 model in the $200 h^{-1}$ Mpc box, the dashed line represents the 128^3 model in the $200 h^{-1}$ Mpc box, and the long-dashed line represents the 128^3 model in the $400 h^{-1}$ Mpc box. The solid line shows a standardized Gaussian, $G(v/\sigma_v)$.

they are constant, independent of the normalization of the power spectrum.

We plot \mathcal{K}_v and \mathcal{K}_g as a function of the Gaussian smoothing radius, R , in Fig. 3. We find that \mathcal{K}_v is close to zero for smoothing between 3 and $15 h^{-1}$ Mpc. In contrast, the gravity field develops a detectable kurtosis. Still, this is substantially less kurtosis than the kurtosis of the gravity’s source field, density. Measured from the high-resolution simulations (i.e. with the grid size 128^3 and the box size of $200 h^{-1}$ Mpc), for the $4 h^{-1}$ Mpc smoothing the density kurtosis is $\mathcal{K}_\delta = 22.2 \pm 5.0$, thus more than an order of magnitude larger than the gravity kurtosis. (For the same smoothing, the kurtosis of the velocity divergence is $\mathcal{K}_\theta = 4.1 \pm 0.6$). Therefore, qualitatively the picture is clear. Our simulations reveal substantially less kurtosis of the velocity and gravity fields than those of the velocity divergence and density contrast respectively; consequently the distributions of v and g are much closer to Gaussian. Our findings are inconsistent with the results of perturbative calculations of Catelan & Moscardini (1994), and consistent with the results of N -body simulations of the velocity field of Kofman et al. (1994).³

³The kurtosis of the velocity field, computed perturbatively by Catelan & Moscardini (1994), is greater than unity already for a Gaussian smoothing scale as large as $10 h^{-1}$ Mpc for all cosmological models they have considered, and grows with decreasing smoothing scale approximately as $\sigma_\delta^2(R)$. In contrast, Kofman et al. (1994) find that ‘the PDF of velocity (...) is almost indistinguishable from Gaussian in the simulations.’

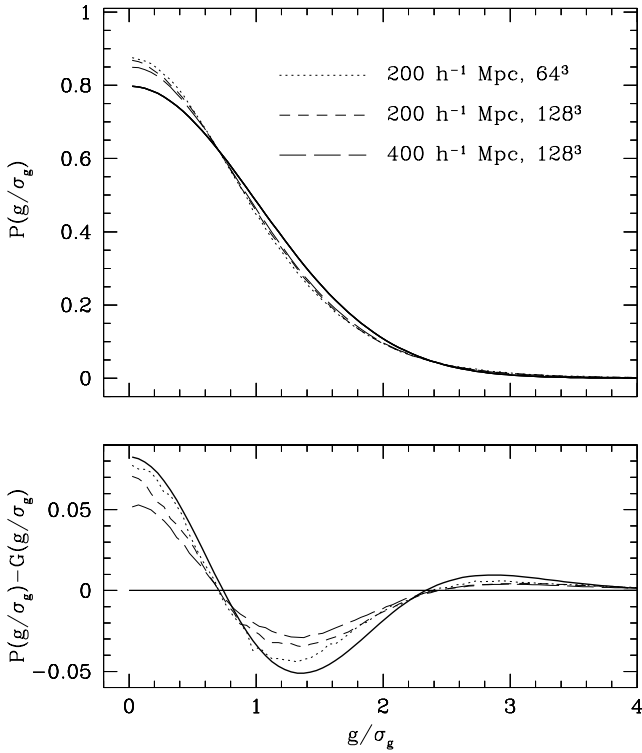


Figure 2. The probability distribution of a Cartesian component of the $4 h^{-1}$ Mpc Gaussian-smoothed gravity field from our simulations and its deviations from Gaussianity. Line coding is the same as in Fig. 1. The thick solid line in the lower panel shows the prediction of equation (11), with $\mathcal{K}_g = \mathcal{S}_{4g} \sigma_\delta^2 = 0.83$.

Quantitatively, the agreement of the evolved velocity and gravity PDFs with the perturbatively motivated equation (11) is less than perfect. In the lower panel of Fig. 2 we plot the difference between the measured distribution for a Cartesian component of the gravity field and the standardized Gaussian. By the thick solid line we plot the difference predicted from equation (11), with the value $\mathcal{K}_g = 0.83$ (the mean value for all models). The predicted difference has too high an amplitude.

Expansion (11) is an expansion in the density variance. In our simulations, for $4 h^{-1}$ Mpc smoothing $\sigma_\delta^2 = 0.65$. For such a large variance, higher-order contributions to formula (11) may simply not be negligible. We have checked this conjecture by analysing the gravity field at an earlier output time. In Fig. 4, we plot the gravity PDF for $\sigma_\delta^2 = 0.25$. Formula (11) fits the simulated distribution better.

We have also checked the perturbative scaling of the gravity (and velocity) kurtosis with the variance of the density field, i.e. equation (12). Although for a given smoothing scale, during weakly non-linear evolution the hierarchical amplitude \mathcal{S}_{4g} remains constant, it depends moderately on the smoothing scale via an effective spectral index of the power spectrum at this scale. However, we have performed an additional simulation for a power-law initial spectrum ($n = -1$), and found qualitatively similar results: a change of sign in the kurtosis at several megaparsecs.

Intrigued by this feature, we have studied the values of the kurtoses for even larger, apparently linear, scales. The results for the gravity kurtosis are shown in Fig. 5. (The results for the velocity kurtosis are similar.) The values of the kurtosis clearly depend on the box size used in the simulations. For the box size equal to

$200 h^{-1}$ Mpc, they tend, instead to zero, to an asymptotic value -1.5 . We interpret this as a purely numerical effect. Namely, on large scales the velocity field of the simulation is dominated by a small number of Fourier waves, and thus the central limit theorem does not force the distribution to be Gaussian, even in the initial conditions. Equations (5) and (6) show that this effect should be much stronger for g than for δ . On the largest scales, approaching the simulation box size, \mathcal{K}_g converges to -1.5 , i.e. the value expected for a single mode, as shown in Appendix A.⁴ On scales shown in Fig. 5, simulations with the $400 h^{-1}$ Mpc box size are much less affected by this effect, as expected.

Why is it that this seems to affect scales down to ~ 20 Mpc? Are there not enough modes, with scales ranging from ~ 20 Mpc to the box size, to warrant Gaussianity? The answer to this question is provided by equation (5). To the variance of the velocity field on a given scale contribute all larger modes with amplitudes proportional to $P(k)$, the density power spectrum. The power spectrum of the APM galaxies, that we have used, has a maximum at $\sim 300 h^{-1}$ Mpc. This is larger than the $200 h^{-1}$ Mpc box size of some of our simulations; thus there are relatively few modes on the scale of the box size that dominate the velocity field on large scales.

To settle this issue definitely would require additional simulations with box size comparable to the Hubble radius (such as the Hubble volume simulations of the VIRGO consortium, (Evrard et al. 2002).⁵ However, the ultimate goal of this paper is to study the relation between velocity and gravity for $4 h^{-1}$ Mpc smoothing. Fig. 3 shows that on such a small scale the velocity and gravity kurtoses are positive, thus most likely induced by non-linear dynamics rather than due to the finite volume of our simulations. However, given the limitations of the Edgeworth expansion,⁶ we would like to have an alternative measure of non-Gaussianity. As such a measure, we borrow the concept of *negentropy* from information theory (e.g. Cover & Thomas 1991; Papoulis 1991).

We define the entropy $S[f]$ of a probability distribution f :

$$S[f] = - \int f(x) \log f(x) dx. \quad (13)$$

It can be shown that, for a given variance, the entropy is maximal for Gaussian fields. Hence the difference between the entropy of a given field and the entropy of a Gaussian of the same variance, the *negentropy* $\mathcal{N}[f]$, can be used as a measure of departure from Gaussianity:

$$\mathcal{N}[f] = S[\text{Gauss}] - S[f]. \quad (14)$$

The negentropy was calculated by numerically integrating the integral of equation (13), using a PDF binned over the range from -5σ to 5σ . We have found that this technique applied to a Gaussian with the same range and binning yielded a negentropy of less than

⁴ As pointed out by Scherrer (private communication), it is straightforward to show that the kurtosis of a Cartesian component of an isotropic gravity field satisfies $\mathcal{K}_g \geq -6/5$, and similarly for the velocity kurtosis. Therefore, any observations which violate this bound indicate that one is in a regime in which the assumption of isotropy breaks down. This occurs in our simulations with the box size of $200 h^{-1}$ Mpc for the smoothing scale of $60 h^{-1}$ Mpc, at which $\mathcal{K}_g < -1.2$ (see Fig. 5). This is consistent with our idea that for such a large smoothing scale, a single mode dominates.

⁵ We have performed an additional simulation with the grid size 256^3 and the box size of $800 h^{-1}$ Mpc. On scales shown in Fig. 5, the gravity kurtosis tended asymptotically to zero, remaining positive.

⁶ The Edgeworth expansion is an asymptotic expansion, not guaranteed to converge. It is not even guaranteed to be positive definite.

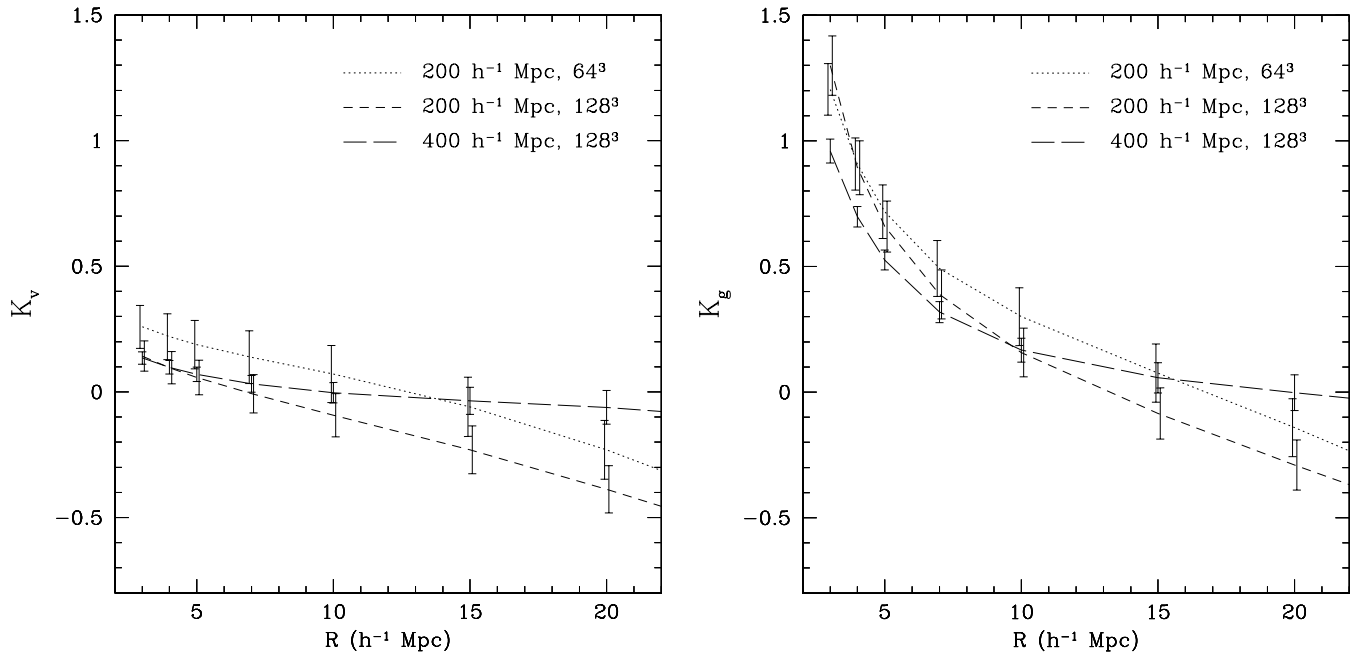


Figure 3. Kurtosis of a Cartesian component of the velocity field (left) and gravity field (right) from our simulations as a function of the Gaussian smoothing length. The points are averages over six simulations times three directions, while the error bars are the standard deviations over this ensemble.

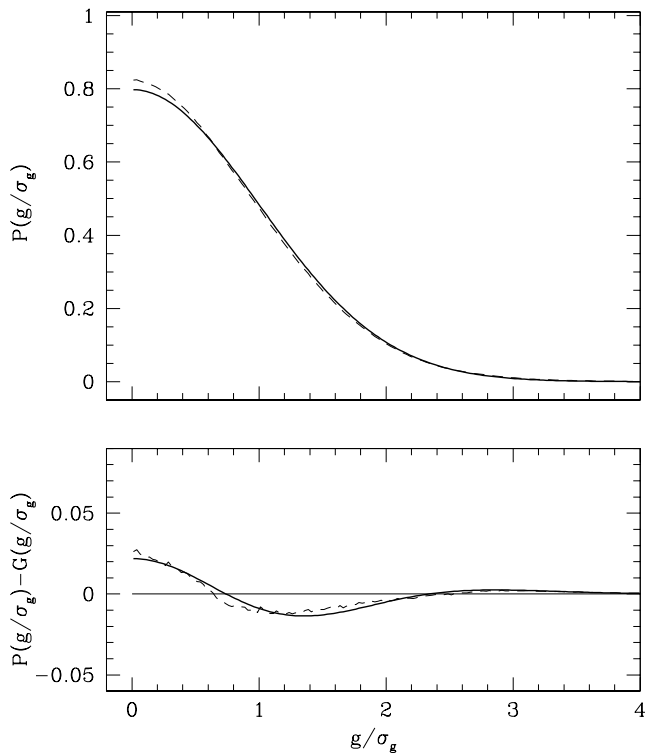


Figure 4. The probability distribution of a Cartesian component of the $4 h^{-1}$ Mpc Gaussian-smoothed gravity field from high-resolution simulations, for $\sigma_g^2 = 0.25$. In the upper panel, the dashed line shows the simulated PDF while the thin solid line represents a standardized Gaussian. In the lower panel, the thick solid line shows the prediction of formula (11), with $K_g = 0.22$.

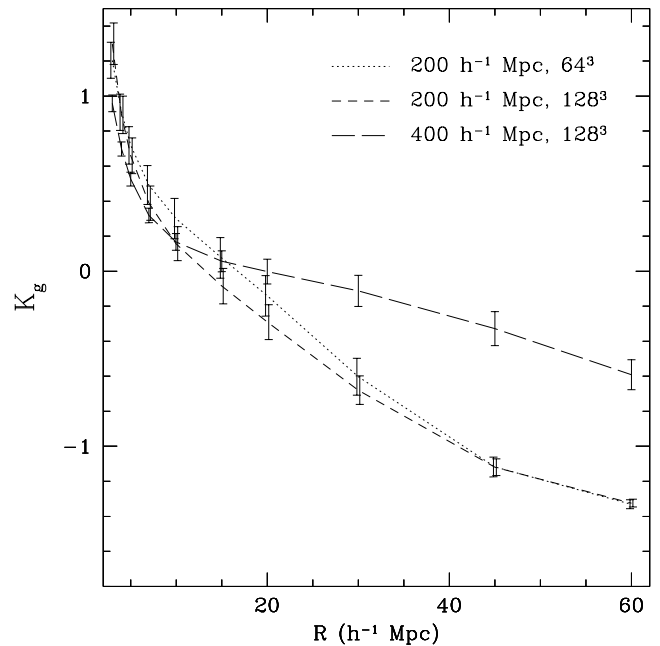


Figure 5. Kurtosis of a Cartesian component of the gravity field from our simulations as a function of the Gaussian smoothing length, now over a larger range of smoothing scales. The points are averages over six simulations times three directions, while the error bars are the standard deviations over this ensemble. Line coding is the same as in Fig. 1. At large scales, the results for simulations with the box size of $200 h^{-1}$ Mpc converge to the same values, regardless the resolution.

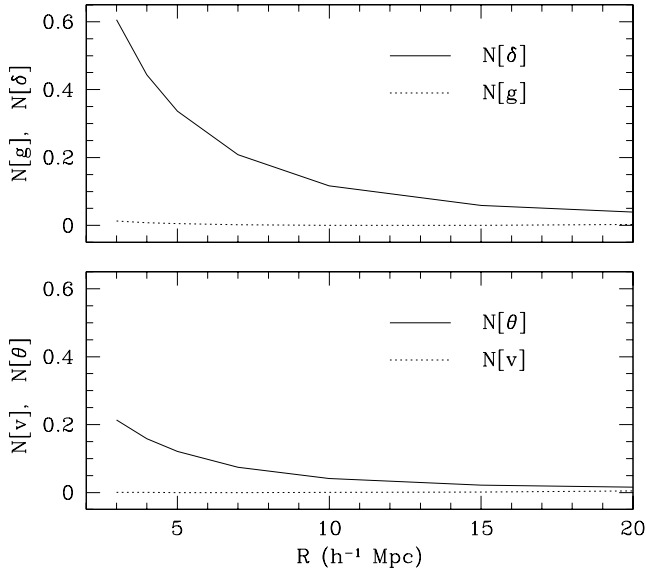


Figure 6. Negentropies of the cosmic fields, for the high-resolution simulations (i.e. with the grid 128^3 and $200 h^{-1}$ Mpc box size). The upper panel compares the negentropies of gravity g and of density contrast δ , and the lower panel compares negentropies of velocity v and of its divergence θ .

10^{-5} , which assures us that our results are not affected by numerical effects.

We plot the results as a function of Gaussian smoothing scale in Fig. 6. The negentropy of the density field is compared to the negentropy of the gravity in the upper panel. The values for velocity and its divergence are compared in the lower panel. The negentropy of the velocity field is practically zero. The negentropy of the gravity field, even on the smallest scales, is extremely small compared to the negentropy of the density. The contrast between the negentropy of the gravity and the negentropy of the density is even greater than between the corresponding kurtoses. This is so because the density field, unlike the gravity field, has significant skewness, also contributing to the value of the negentropy. In other words, the density field is more non-Gaussian than the gravity field not only because it has larger kurtosis, but also because it has non-vanishing skewness.

We conclude that on mildly non-linear scales, the non-Gaussianity of v and g is completely negligible compared to the non-Gaussianity of θ and δ . As stated earlier, this finding is consistent with the results of N -body simulations of the velocity field of Kofman et al. (1994). It is also consistent with the results of Gooding et al. (1992) and Scherrer (1992), where non-Gaussianity of the density field was (at least on large scales) due to initial conditions rather than non-linear gravitational evolution.

4 THE ONE-COMPONENT v - g RELATION

In grid simulations, the shortest Fourier modes correspond to the Nyquist wavelength, of two cells. Smaller structures are not well resolved by the code. In low-resolution simulations (cell size $3.13 h^{-1}$ Mpc, see Table 1), the Nyquist wavelength is larger than the scale at which we would like to study the velocity–gravity relation ($4 h^{-1}$ Mpc). In high-resolution simulations (cell size $1.56 h^{-1}$ Mpc), it is smaller. Therefore, to model the velocity–gravity relation at $4 h^{-1}$ Mpc scale, we use only high-resolution simulations.

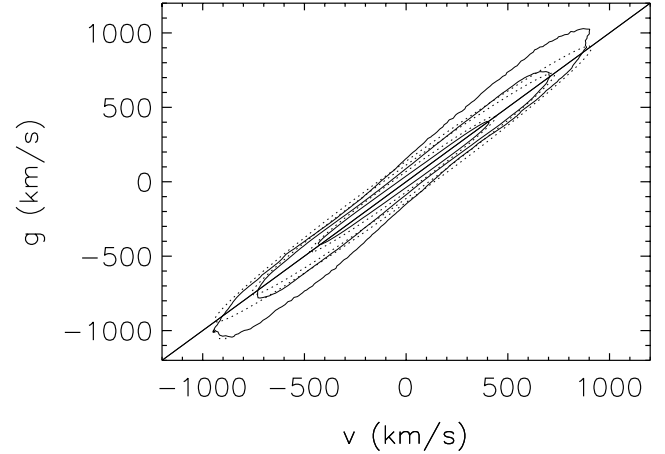


Figure 7. The joint probability distribution of a Cartesian component of the cosmic velocity and gravity fields, both smoothed with a $4 h^{-1}$ Mpc Gaussian filter. Solid contours represent combined numerical results from six high-resolution simulations, and dotted contours represent a standardized bivariate Gaussian of the same correlation coefficient. The contours correspond to the probability levels of 68, 95 and 99 per cent.

On scales of a few h^{-1} Mpc, the relation between δ and θ is non-linear. Nevertheless, because the probability distributions of the Cartesian components of both v and g are nearly Gaussian, we hypothesize that their joint probability distribution is a (bivariate) Gaussian as well. In Fig. 7 we present the simulated joint PDF for v and g , measured on the $4 h^{-1}$ Mpc scale. It is indeed quite close to a bivariate Gaussian. The only substantial deviation is for the probability contour of 99 per cent, along the gravity coordinate. There, positive kurtosis of the gravity field broadens the simulated isocontour with respect to the Gaussian one. Fig. 7 also shows that v and g are strongly correlated. In Appendix B we show that, in the bivariate Gaussian case, the relationship between v and g is purely linear; we now show that this is approximately the case in the simulations.

In the linear regime $v = g$ and thus each of the Cartesian components of these quantities, which we denote v and g , respectively, are also equal. In practice, the relationship between these two quantities has some finite scatter (Fig. 7), thus we characterize the relation between the mean v at constant g , $\langle v | g \rangle$, and the converse, $\langle g | v \rangle$. Fitting a straight line to $\langle v | g \rangle$ as a function of g gives a slope of 0.94. Therefore, assuming pure linear theory on this scale would give a systematic 6 per cent error in β . We now consider going beyond linear theory.

The relationship between $\langle v | g \rangle$ and g should be invariant to coordinate inversions, thus it must be an odd function; similarly for the relationship between $\langle g | v \rangle$ and v .

Hence, we adopt third-order polynomials

$$\langle g | v \rangle = c_1 v + c_3 v^3 / \sigma_v^2 \quad (15)$$

$$\langle v | g \rangle = d_1 g + d_3 g^3 / \sigma_g^2 \quad (16)$$

as the simplest odd non-linear model, and we use the unitless parameters c_3 and d_3 as a measure of the non-linearity of the relation. As the deviations from linear theory are small, we expect c_1 and d_1 to be close to unity, and c_3 and d_3 to be small. Because in velocity–velocity comparisons we reconstruct velocities based on the gravity field, the quantity $\langle v | g \rangle$ is more relevant, and we concentrate on it in this paper. Note, however, that relation (15) can be used to

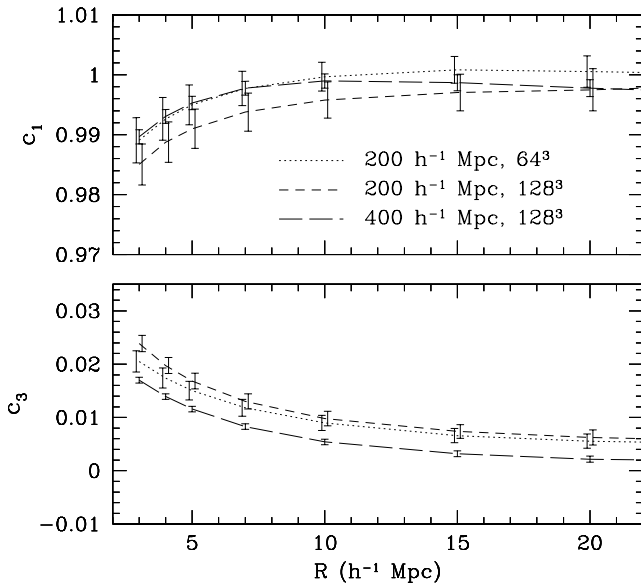


Figure 8. The parameters c_1 and c_3 of the polynomial approximation to the mean one-component v - g relation (equation 15) as functions of the smoothing scale. Line coding is the same as in Fig. 1.

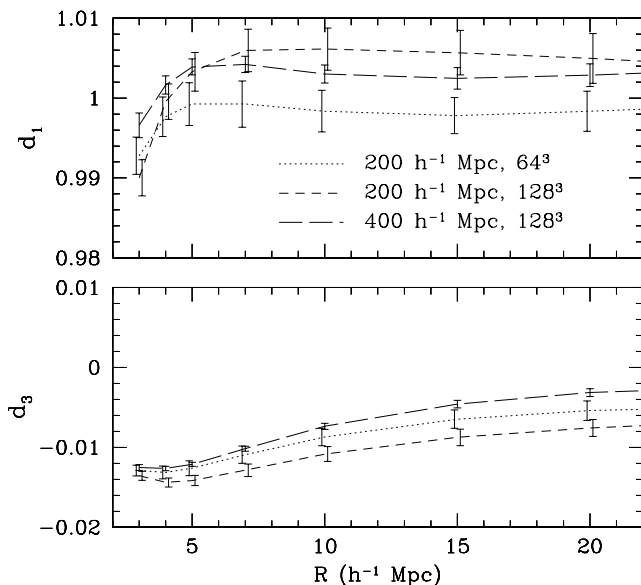


Figure 9. The parameters d_1 and d_3 of the polynomial approximation to the mean one-component g - v relation (equation 16) as functions of the smoothing scale. Line coding is the same as in Fig. 1.

transform velocities in the first step of density–density comparisons such as POTENT (Dekel et al. 1999).

The parameters c_1 and c_3 as functions of the smoothing scale are shown in Fig. 8, while Fig. 9 shows d_1 and d_3 . We have fitted them independently for the three coordinates in each of the six realizations of every numerical model; the lines are the averages over these 18 data sets and error bars indicate their standard deviations. As expected, c_3 and d_3 are much smaller than unity. On large scales, c_1 and d_1 tend to the linear theory value with accuracy better than half a per cent. Moreover, they remain close to unity even on small scales, which implies that the systematic bias in estimating β based on the linear theory approximation (2) is small.

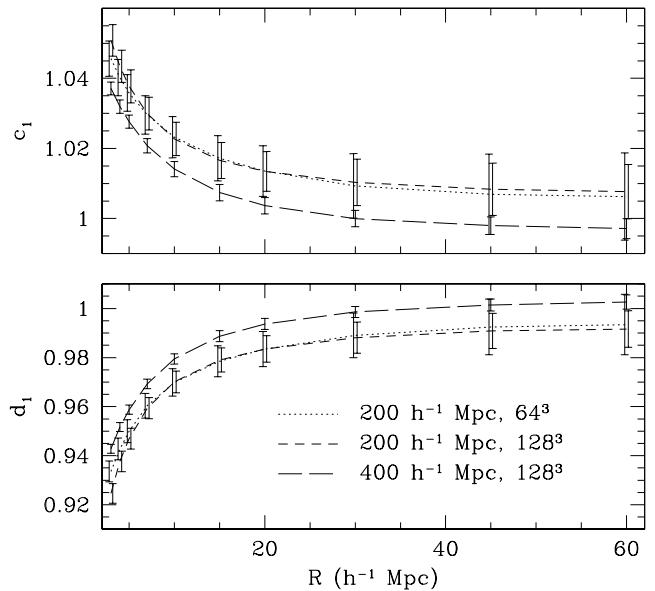


Figure 10. The parameters c_1 and d_1 when the parameters c_3 and d_3 are set to zero. Line coding is the same as in Fig. 1.

To quantify this bias, in Fig. 10 we show the parameters c_1 and d_1 when c_3 and d_3 are set to zero. For $R > 20 h^{-1} \text{ Mpc}$, c_1 and d_1 deviate from unity by less than 2 per cent. Therefore, at these scales we can apply linear theory with good accuracy.

Note in Figs 8 and 9 that, at small scales, high-resolution simulations yield the highest values of c_3 and $1 - c_1$ (similarly for $|d_3|$ and $1 - d_1$), but overall the effects of resolution and of the simulation box size are not large.

We plot the mean predicted velocity as a function of the true velocity for a $4 h^{-1} \text{ Mpc}$ Gaussian filter in Fig. 11. The velocity predicted with the linear-theory model (i.e. the gravity) is plotted as a dashed line. Combined data from six realizations of our high-resolution model (three components each) are binned with respect to the predicted velocity and averaged in the bins. All velocities are in kilometres per second (the one-dimensional rms true velocity $\sigma_v = 290 \text{ km s}^{-1}$ on this scale). A long-dashed line shows the velocity predicted by the polynomial formula (16). We see that linear theory, $v = g$, is a good fit for velocities up to about $2\sigma_v$. The polynomial approximation works well up to about $3\sigma_v$, but also fails in the tails. Therefore, we decided to seek a better estimator of velocity from density than a simple function of gravity.

KCPR have found that formula (8) is a good description of the tails of the relation between the density and the velocity divergence, so it should also work well on the integral level (equation 10). It turns out, however, that at small scales a small modification is needed. Formula (8) implies that the coefficient of the linear term in density in the density–velocity divergence relation is unity, $\theta_\delta = \delta - r_2(\delta^2 - \sigma_\delta^2) + \dots$, where $r_2 = (\alpha - 1)/2\alpha$, regardless of the value of α , while we have found here that at small scales it is not strictly true. To cure this problem, we introduced an additional parameter, γ , so that

$$\theta_\delta = \alpha\gamma[(1 + \delta)^{1/\alpha} - 1] + \epsilon. \quad (17)$$

For given α and γ the predicted velocity, v_{pred} , was calculated from equation (10). The best values of α and γ were found by minimizing the quantity $X^2 \equiv \sum_i (v_{\text{pred}}^{(i)} - v_{\text{true}}^{(i)})^2 / (3N^3)$, where v_{true} is the true velocity and the sum is over all grid points (N^3 in total) and all Cartesian components. The resulting values of the parameters, for

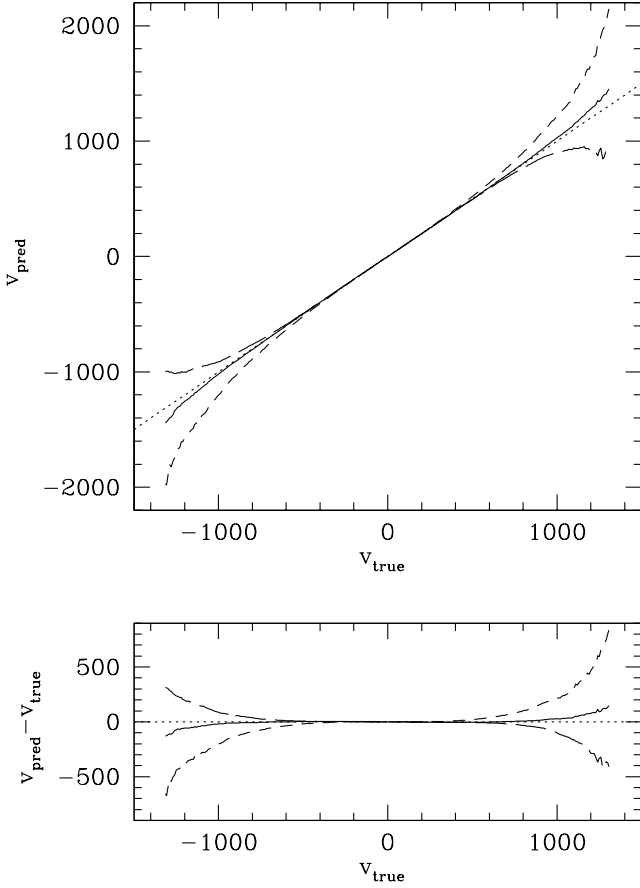


Figure 11. One Cartesian component of the velocities reconstructed from the density field – combined data from six high-resolution simulations, observed with a $4 h^{-1}$ Mpc Gaussian filter. Top: mean predicted velocity given true velocity. Bottom: errors of the reconstruction. All velocities are in kilometres per second. The one-dimensional rms true velocity, σ_v , for this smoothing equals 290 km s^{-1} . The dotted line denotes identity; the dashed line, linear theory model; the long-dashed line, a polynomial model (equation 16). The solid line shows the reconstruction from the density field computed using the non-linear $\alpha\gamma$ -formula (equation 17), with $\alpha = 1.56$ and $\gamma = 1.054$.

the smoothing scale $4 h^{-1}$ Mpc and different values of σ_8 at different output times, are shown in Fig. 12.

In the limit of linear theory, $\alpha = \gamma = 1$. The offset ϵ , fully determined by α and γ , is then equal to zero. In general, on the integral level the value of ϵ is irrelevant, as its contribution to velocity in the integral in equation (10) averages out to zero. We see that for small σ_8 the parameter γ tends to unity, while α decreases only weakly and remains well away from this value. This is consistent with the findings of KCPR, that the α -formula – equations (8) or (17) with $\gamma = 1$ – describes well the density–velocity relation in the weakly non-linear regime (i.e. for σ_8 smaller than, say, 0.3). Though the best-fitting value of γ is close to unity even for large σ_8 , its inclusion markedly decreases X^2 .

In Fig. 13 we plot the quantity $\chi(v) \equiv \sqrt{\Delta X^2 / \Delta N}$, that is, the square root of the contribution to X^2 from a given bin in velocity, divided by the number of points in that bin. (χ has units of km s^{-1} .) We have $X^2 = \int \chi^2(v) P(v) dv$, where $P(v)$ is the PDF of a Cartesian component of the velocity field. Thus, X^2 is a number-weighted average of χ^2 . The dashed line shows χ for the velocity predicted according to the linear theory, the long-dashed line denotes the ve-

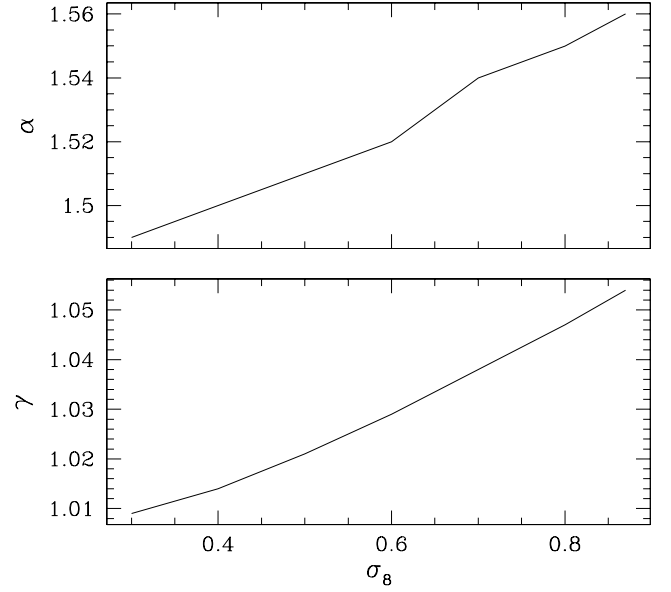


Figure 12. The parameters α and γ of formula (17) for $4 h^{-1}$ Mpc Gaussian smoothing, as functions of σ_8 .

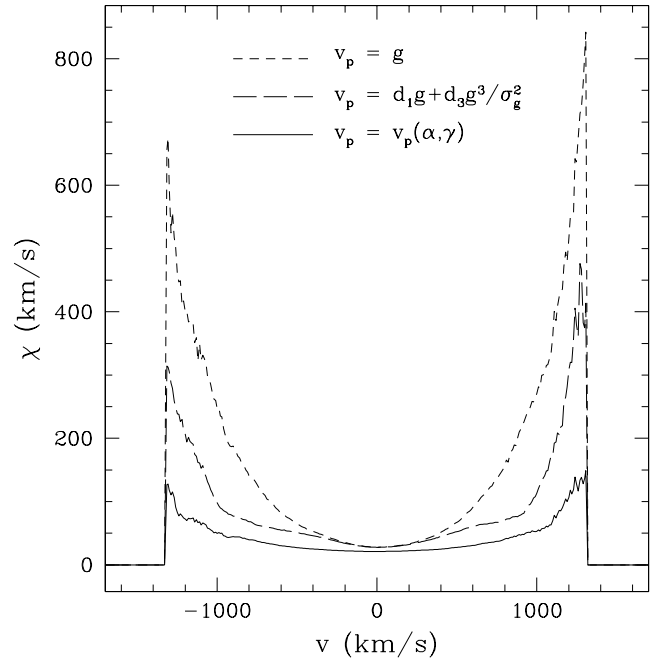


Figure 13. The quantity χ (see text): the dashed line shows it for the velocity predicted according to the linear theory; long-dashed, for the velocity approximated by a polynomial in the gravity; and solid, for the velocity predicted by the $\alpha\gamma$ -formula, inserting equation (17) into equation (10).

locity approximated by a polynomial in the gravity, and the solid line represents the velocity predicted by the $\alpha\gamma$ -formula, inserting equation (17) into equation (10). The linear-theory estimator of velocity yields the largest values of χ . The polynomial formula results in smaller χ in the tails, but in equal χ for ‘typical’ values of velocity ($-\sigma_v \leq v \leq \sigma_v$). The $\alpha\gamma$ -formula yields the smallest χ in the whole range of velocity. For typical values of velocity, i.e. where most of

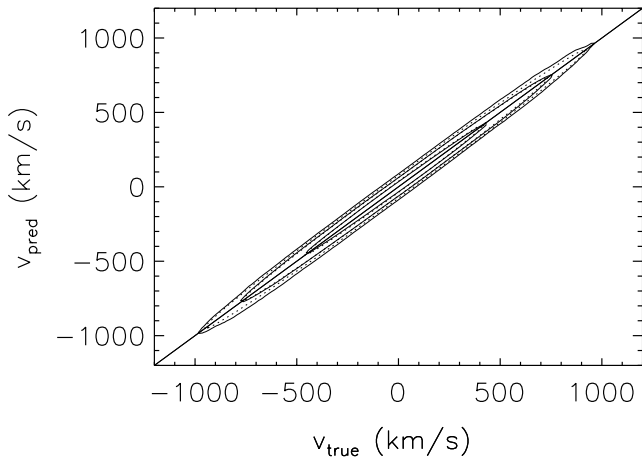


Figure 14. The joint probability distribution of a Cartesian component of the velocity predicted by the $\alpha\gamma$ -formula and the true velocity, both smoothed with a $4 h^{-1}$ Mpc Gaussian filter. Solid contours represent combined numerical results from six high-resolution simulations, and dotted contours represent a bivariate Gaussian of the same correlation coefficient and variances. The contours correspond to the probability levels of 68, 95 and 99 per cent.

the data comes from, χ is slightly smaller than for the previous estimators. Furthermore, it grows only moderately in the tails.

In Fig. 11, a solid line shows the mean velocity predicted by the $\alpha\gamma$ -formula as a function of the true velocity. The smoothing scale is that of VELMOD, i.e. $4 h^{-1}$ Mpc, and $\sigma_8 = 0.87$. For this value of σ_8 , the best-fitting values of α and γ are $\alpha = 1.56$ and $\gamma = 1.054$. We see that the $\alpha\gamma$ -formula yields a practically unbiased estimator of velocity. The difference between the predicted and true velocity in the tails is very small.

Fig. 14 demonstrates that the estimator of velocity from density provided by the $\alpha\gamma$ -formula is not only essentially unbiased but also has a small variance (as suggested already by Fig. 13). The figure shows a joint PDF for the velocity predicted by the $\alpha\gamma$ -formula and the true velocity, for $4 h^{-1}$ Mpc smoothing. It is instructive to compare it with Fig. 7, where $v_{\text{pred}} = g$. We have found that, for larger values of the smoothing scale, the correlation between the predicted and true velocity is even higher.

In Fig. 15 we show the dependence of α and γ on the smoothing scale, for $\sigma_8 = 0.87$. For large R the parameter γ tends to unity, as expected. The parameter α grows from the value around 1.55 for $3 h^{-1}$ Mpc, to around 2.05 for $20 h^{-1}$ Mpc. This is in contrast with the results of KCPR, where $\alpha \simeq 1.9$ was a good fit for a large range of scales. We can see at least three likely sources of this discrepancy. First, the power spectrum used by KCPR was a pure power law, $P(k) \propto k^{-1}$, while ours is not and the effective spectral index of our APM spectrum depends (slightly) on the smoothing scale. Secondly, KCPR studied the α -formula, equation (8), which is equivalent to our $\alpha\gamma$ -formula only when $\gamma = 1$. Finally, the fit of KCPR was obtained for all bins in velocity having equal weight, while we weight the bins by the number of points. As a result, our fit is much less affected by the tails of the velocity distribution.

To summarize, we have tested various estimators of velocity from density. Non-linear effects can be accounted for either at the integral level, employing equation (16), or at the differential level, employing equation (17). We have shown that the differential method works much better.

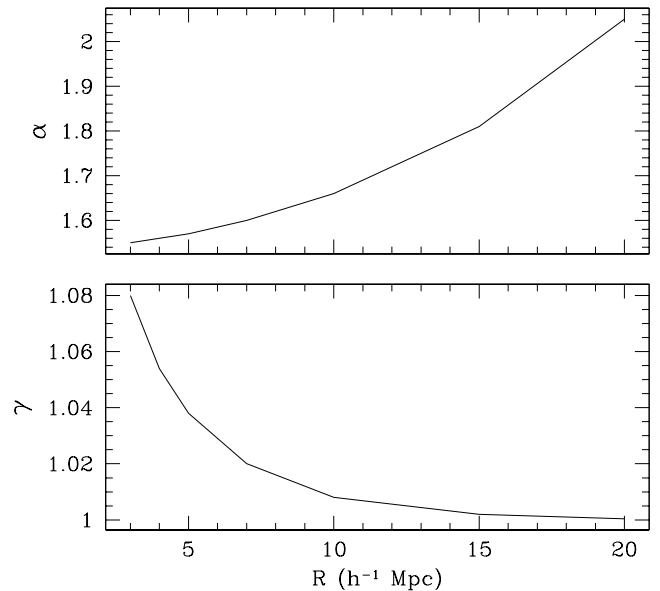


Figure 15. The dependence of α and γ on the smoothing scale, for $\sigma_8 = 0.87$.

5 SUMMARY AND CONCLUSIONS

In this paper, we have studied the cosmic velocity–gravity relation. First, we have measured the non-Gaussianities of the cosmic velocity and gravity fields, evolved from Gaussian initial conditions, by computing their kurtoses and negentropies. We have shown that, on scales of a few h^{-1} Mpc, the non-Gaussianities of the cosmic velocity and gravity fields are small compared to the non-Gaussianities of velocity divergence and density. A similar finding for the velocity field was reported by Kofman et al. (1994). Guided by this result, we have shown that the relation between v and g is nearly linear. Moreover, its proportionality coefficient is close to that predicted by linear theory. Specifically, we have shown that the systematic errors in velocity–velocity comparisons due to assuming linear theory do not exceed 6 per cent in β . (Strictly speaking, if $\sigma_8 < 0.9$ and the smoothing scale is no smaller than $4 h^{-1}$ Mpc). To correct for this small bias, we have tested various non-linear estimators of velocity from density. We have shown that the $\alpha\gamma$ -formula (a slight modification of the α -formula proposed by KCPR) yields an estimator which is essentially unbiased and of small variance.

The smoothing of observed peculiar velocity data, with its sparse and noisy coverage of the velocity, is technically difficult. Thus velocity–velocity analyses such as VELMOD compare unsmoothed peculiar velocities with minimally smoothed predicted velocity fields from redshift surveys. The finite resolution of a grid code does not allow us to test this effect; it would be worthwhile to repeat the calculations with a high resolution N -body code, or with CPPA enhanced with adaptive mesh refinement. The former has been performed by Berlind et al. (2000), but they did not separate the effects of non-linear evolution from the effects of different smoothing of the velocity and gravity fields.

An alternative method of estimating β from cosmic velocities is to compare the cosmic microwave background dipole with the density dipole inferred from a galaxy redshift survey. In maximum-likelihood approaches to this problem (Strauss et al. 1992; Schmoltd et al. 1999; Chodorowski & Cieliegg, in preparation) the relevant quantity is the joint distribution for the velocity and gravity, which is commonly approximated as a multivariate Gaussian. We have

shown that this indeed holds to fairly good accuracy (Fig. 7). Small non-linear effects can be corrected for by a more thorough modelling of the joint distribution. There is, however, a better approach. From a redshift survey, instead of calculating the acceleration on the Local Group (i.e. the density dipole, or gravity), we can calculate the predicted velocity from the $\alpha\gamma$ -formula. The joint distribution for the predicted velocity and the true velocity is perfectly Gaussian (see Fig. 14). Moreover, the relation between these two variables is tighter than the relation between the velocity and the gravity. This implies that, in the proposed method, the estimated value of β will be unbiased and its inferred errors will be smaller.

ACKNOWLEDGMENTS

We thank Tomek Plewa for his contribution to the numerical code we have used and Michał Różyczka for fruitful and animating discussions. This research has been supported in part by the Polish State Committee for Scientific Research grants, Nos 2.P03D.014.19 and 2.P03D.017.19, and NSF grant AST96-16901. The simulations were performed at the Interdisciplinary Centre for Mathematical and Computational Modelling, Pawińskiego 5A, PL-02-106, Warsaw.

REFERENCES

- Baugh C. M., Efstathiou G., 1993, MNRAS, 265, 145
 Baugh C. M., Efstathiou G., 1994, MNRAS, 267, 323
 Baugh C. M., Gaztañaga E., 1996, MNRAS, 280, L37
 Berlind A. A., Narayanan V. K., Weinberg D. H., 2000, ApJ, 537, 537
 Bernardeau F., 1992, ApJ, 390, L61
 Bernardeau F., Kofman L., 1995, ApJ, 443, 479
 Bernardeau F., Chodorowski M. J., Łokas E. L., Stompor R., Kudlicki A., 1999, MNRAS, 309, 543
 Catelan P., Moscardini L., 1994, ApJ, 436, 5
 Chodorowski M. J., 1997, MNRAS, 292, 695
 Chodorowski M. J., Łokas E. L., 1997, MNRAS, 287, 591
 Chodorowski M. J., Łokas E. L., Pollo A., Nusser A., 1998, MNRAS, 300, 1027
 Colella P., Woodward P. R., 1984, J. Comput. Phys., 54, 174
 Cover T. M., Thomas J. A., 1991, Elements of Information Theory. Wiley, New York
 Davis M., Strauss M. A., Yahil A., 1991, ApJ, 372, 394
 Davis M., Nusser A., Willick J. A., 1996, ApJ, 473, 22
 Dekel A., Eldar A., Kolatt T., Yahil A., Willick J. A., Faber S. M., Courteau S., Burstein D., 1999, ApJ, 522, 1
 Eke V. R., Cole S., Frenk C. S., 1996, MNRAS, 282, 263
 Evrard A. E. et al., 2002, ApJ, 573, 7
 Gooding A. K., Park C., Spergel D. N., Turok N., Gott III R., 1992, ApJ, 393, 42
 Gramann M., 1993, ApJ, 405, L47
 Juszkiewicz R., Weinberg D. H., Amsterdamski P., Chodorowski M. J., Bouchet F. R., 1995, ApJ, 442, 39
 Kofman L., Bertschinger E., Gelb J. M., Nusser A., Dekel A., 1994, ApJ, 420, 44
 Kudlicki A., Plewa T., Różyczka M., 1996, Acta A., 46, 297
 Kudlicki A., Chodorowski M. J., Plewa T., Różyczka M., 2000, MNRAS, 316, 464 (KCPR)
 Lahav O., Lilje P. B., Primack J. R., Rees M. J., 1991, MNRAS, 251, 128
 Longuet-Higgins M. S., 1963, J. Fluid Mech., 17, 459
 Mancinelli P. J., Yahil A., 1995, ApJ, 452, 75
 Mancinelli P. J., Yahil A., Ganon G., Dekel A., 1994, in Bouchet F. R., Lachièze-Rey M., eds, Proc. 9th IAP Astrophysics Meeting, Cosmic Velocity Fields. Editions Frontières, Gif-sur-Yvette, p. 215
 Nusser A., Colberg J. M., 1998, MNRAS, 294, 457
 Nusser A., Dekel A., Bertschinger E., Blumenthal G. R., 1991, ApJ, 379, 6
 Papoulis A., 1991, Probability, Random Variables, and Stochastic Processes. 3rd edn. McGraw-Hill, New York
 Peebles P. J. E., 1980, The Large-scale Structure of the Universe. Princeton Univ. Press, Princeton, NJ
 Rowan-Robinson M. et al., 2000, MNRAS, 314, 375
 Saunders W. et al., 2000, MNRAS, 317, 55
 Scherrer R., 1992, ApJ, 390, 330
 Schmoltdt I. et al., 1999, MNRAS, 304, 893
 Scoccimarro R., Colombi S., Fry J. N., Frieman J. A., Hivon E., Melott A., 1998, ApJ, 496, 586
 Strauss M. A., Willick J. A., 1995, Phys. Rep., 261, 271
 Strauss M. A., Yahil A., Davis M., Huchra J. P., Fisher K., 1992, ApJ, 397, 395
 Willick J. A., Strauss M. A., 1998, ApJ, 509, 64
 Willick J. A., Strauss M. A., Dekel A., Kolatt T., 1997, ApJ, 486, 629

APPENDIX A: CALCULATION OF THE KURTOSIS OF VELOCITY FOR A SINGLE FOURIER MODE

Let us assume a single-mode distribution of the density field. All variables will depend on one dimension only. In the linear regime the density field is

$$\delta(x, y, z) = \delta(x) = \sin(x). \quad (\text{A1})$$

(The amplitude of the wave is irrelevant here, as it will cancel out in the calculation of the dimensionless kurtosis.) Then, in the linear regime,

$$\delta = \theta = -\nabla \cdot \mathbf{v} = -\frac{dv}{dx}. \quad (\text{A2})$$

[θ denotes the scaled velocity divergence, so in equation (A2) there is no $f(\Omega_m, \Omega_\Lambda)$ term.] Hence,

$$v = -\int \delta(x) dx \quad (\text{A3})$$

and

$$v(x) = \cos(x). \quad (\text{A4})$$

Let $P(v)$ denote the volume-weighted PDF of a single component of the velocity field:

$$P(v)|dv| = \frac{1}{\pi}|dx|. \quad (\text{A5})$$

Hence,

$$P(v) = \frac{1}{\pi \sin(x)} = \frac{1}{\pi \sqrt{1 - \cos^2(x)}}, \quad (\text{A6})$$

and finally

$$P(v) = \pi^{-1}(1 - v^2)^{-1/2}. \quad (\text{A7})$$

Now let us compute the four first moments of this distribution:

$$\langle v \rangle = 0 \quad (\text{A8})$$

$$\langle v^2 \rangle = \frac{1}{\pi} \int_{-1}^1 \frac{v^2 dv}{\sqrt{1 - v^2}} = \frac{1}{2} \quad (\text{A9})$$

$$\langle v^3 \rangle = 0 \quad (\text{A10})$$

$$\langle v^4 \rangle = \frac{1}{\pi} \int_{-1}^1 \frac{v^4 dv}{\sqrt{1 - v^2}} = \frac{3}{8}. \quad (\text{A11})$$

We can calculate the kurtosis of this field now:

$$K_v = \frac{\langle v^4 \rangle - 3\langle v^2 \rangle^2}{\langle v^2 \rangle^2} = -\frac{3}{2}. \quad (\text{A12})$$

APPENDIX B: THE MEAN RELATION BETWEEN TWO GAUSSIAN VARIABLES

Consider two correlated Gaussian variables, y_1 and y_2 , with zero means and variances $\sigma_1^2 \equiv \langle y_1^2 \rangle$ and $\sigma_2^2 \equiv \langle y_2^2 \rangle$, respectively. Their correlation coefficient is

$$r \equiv \frac{\langle y_1 y_2 \rangle}{\sigma_1 \sigma_2}. \quad (\text{B1})$$

Let us introduce normalized variables, $\mu \equiv y_1/\sigma_1$ and $\nu \equiv y_2/\sigma_2$. We require that their joint PDF is a bivariate Gaussian,

$$p(\mu, \nu) = \frac{1}{2\pi\sqrt{1-r^2}} \exp \left[-\frac{(\mu^2 - 2r\mu\nu + \nu^2)}{2(1-r^2)} \right]. \quad (\text{B2})$$

Were the fields uncorrelated ($r = 0$), $p(\mu, \nu)$ would be just a product of two Gaussian distributions of μ and ν .

Because the variables are assumed to be correlated but in general not identical, the relation between them will have a scatter. The mean relation between μ and ν is defined as mean μ given ν , $\langle \mu | \nu \rangle$. By definition, the conditional PDF of μ given ν , $p(\mu | \nu)$, is $p(\mu, \nu)/p(\nu)$. Equation (B2) yields

$$p(\mu | \nu) = \frac{1}{\sqrt{2\pi(1-r^2)}} \exp \left[-\frac{(\mu - r\nu)^2}{2(1-r^2)} \right]. \quad (\text{B3})$$

We see that the conditional PDF is a Gaussian with modified mean and variance. Specifically,

$$\langle \mu | \nu \rangle = r\nu, \quad (\text{B4})$$

and

$$\langle \mu^2 | \nu \rangle - \langle \mu | \nu \rangle^2 = 1 - r^2. \quad (\text{B5})$$

The relation between two correlated Gaussian variables is thus linear. If the variables are uncorrelated there is no relation whatsoever.⁷ Therefore, the relation between two Gaussian variables, if it exists at all, is always linear.

We may define an ‘inverse’ relation to that specified in equation (B4), i.e. $\langle \nu | \mu \rangle$. From symmetry of the joint PDF,

$$\langle \nu | \mu \rangle = r\mu. \quad (\text{B6})$$

The proportionality coefficient in the ‘inverse’ relation is thus not a simple reciprocal of the coefficient in the ‘forward’ relation, equation (B4). The difference is equal to $(1-r^2)/r \simeq 1-r^2$ for r close to unity. In other words, the difference between the true and the ‘naive’ coefficient of the inverse relation is directly related to the scatter in the relation.

⁷This is only the case for Gaussian variables. For a counterexample in the opposite case, consider y_1 and $y_2 = y_1^2$, where y_1 is Gaussian.